PERIODICA POLYTECHNICA SER. MECH. ENG. VOL. 42, NO. 1, PP. 33–45 (1998)

JET-INDUCED FLOW IN CYLINDRICAL TANKS I. VISUALIZATION AND MODELLING

I. TUWEGIAR and Elemér LITVAI

Department of Fluid Dynamics
Technical University of Budapest
H–1521 Budapest, Hungary

Received: December 10, 1996

Abstract

The flow field induced by a submerged inclined jet in a cylindrical tank is treated. A flow visualization and velocity measurement on the free surface of the tank delineated a simple constant eddy viscosity axisymmetric model that may be used to predict the flow field in the tank. A formula for the prediction of the tangential velocity on the free surface of the tank was deduced from the Navier-Stokes equations and balances of the radial momentum. Thus, the whole flow field may be predicted from design and operational parameters.

Keywords: submerged, monophase, floating particles, free surface, mean swirl velocity, constant eddy viscosity, prediction from design and operational parameters.

1. Introduction

A vortex with an axial velocity component is generally called swirling flow. Such flow configuration exists in many industrial devices; cyclone separators, hydrocyclone separators, swirling spray dryers, swirling furnaces and vortex tubes used for thermal separation. It can be found also in agitated chemical tanks and turbo-machinery passages and piping.

The swirling flow in these devices is mostly regarded as a turbulent one, where fluid fluctuations are occurring in all: tangential, radial and axial directions. Usually the tangential velocity component strongly dominates the state of swirling flow. KURODA and OGAWA [9] reviewed turbulent swirling pipe flow and explained the available methods for correlating the mean swirl velocity $\overline{V}_\theta$. The flow domain is divided into two regions (*Fig. 1*), i.e. forced rotational flow in the center of the pipe, and quasi-free rotational flow surrounding it. Typical empirical expressions used for modelling and data fitting of $\overline{V}_\theta$ distributions are:

1. Transformation of Rankine's compound vortex

$$\overline{V}_\theta = \omega_s r^n \tag{1.1}$$

for the forced vortex,

$$\overline{V}_\theta = \frac{\omega_s r_b^{n+m}}{r^m} \tag{1.2}$$

for quasi-free vortex.

2. Transformation of Burgers vortex

$$\overline{V}_\theta = \frac{k_1}{r}\left(1 - e^{-k_2 r^2}\right), \tag{2}$$

where k_1, k_2, r_b (defined in *Fig. 1*), m, n and ω_s (characteristic angular velocity in the forced vortex) are to be determined from experiment. Since their values depend on local flow conditions, it is difficult to determine them from operational conditions. On the other hand, it is important from engineering point of view to establish how to estimate $\overline{V}_\theta$ distribution for an arbitrary operational condition. KURODA and OGAWA [9] used the transformation of Rankine's compound vortex to model swirling flow in a pipe. Their model depends on r_b and $\overline{V}_{\theta b}$ which can be found only by experiment.

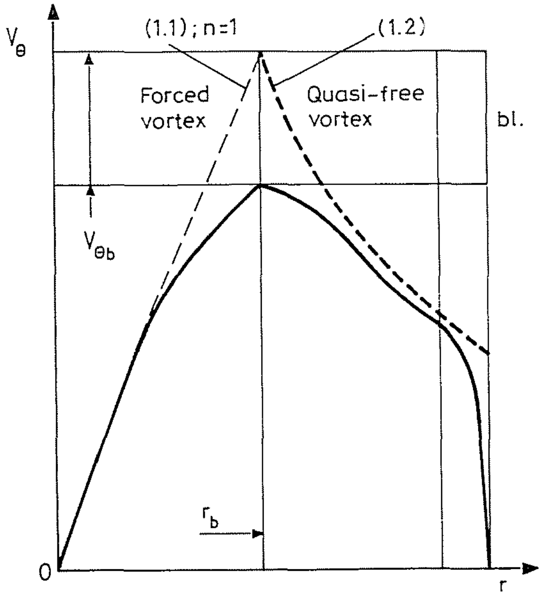

Fig. 1. Theoretical tangential velocity distribution

The transformation of Burgers' vortex was derived by BURGERS [2] to explain the mechanism of turbulence. Later, it was independently derived by ROTT [8]. He used it to model stagnation point flow and to explain some practical physical phenomena such as flow in the bath tub, the tornado problem and the phenomena found at the intake of jet engines situated (at rest) near the ground.

In equilibrium, a 'viscous radius', r^* is found which is determined by the kinematic viscosity ν and the gradient of the incoming flow a:

$$r^* = \sqrt{\frac{2\nu}{a}}. \tag{3}$$

To alleviate the restriction of a stagnation flow extending to infinity, Rott proposes that the viscous effect is restricted to a cylinder of radius of the order of r^*; thus, the solution can be applied, in the sense of a boundary-layer approximation, to the core of any vortex aligned with an axisymmetric stagnation point whatever the flow at infinity may be. Subsequently, Burgers' transformation has been used [3] as the basis for comparison of swirl-velocity measurements for numerous practical devices such as those mentioned previously. *Eq.* (13) was utilized despite the assumption of uniform axial velocity which,as experiment indicates, is far from real. Also, in most practical situations, the vortex core is turbulent and so an eddy viscosity ν_e has been substituted for the kinematic viscosity.

In modern chemical processing units, it is common practice for liquids in a tank to be circulated by drawing them through a pump and returning them to the tank through a pipe or a nozzle for such purposes as homogenization of physical properties, prevention of stratification, prevention of deposition of suspended particles and tank cleaning. The problem under investigation here has similar arrangement with application to waste treatment.

The setup used for both numerical and experimental simulations is shown in *Fig. 2.* It consists of a cylindrical tank with flat bottom equipped with a nozzle, pump and connecting hoses. Water leaves the tank via four peripheral outlets. The nozzle can be positioned at the desirable location and angle. A similar setup is being used in a waste treatment plant in Hungary to stir aeration tanks in order to keep matter suspended. Our model contains only pure water and no air. When the nozzle is inclined and positioned away from the centre of the tank, the flow is turbulent and three-dimensional. In this case the problem has the following features:

- The flow field is described by the 3D Navier-Stokes equations which are coupled high-order non-linear partial differential equations. Their solution is a challenge to the most powerful computational methods and computers.
- The flow is turbulent and the addition of a turbulence model such as the $k-\varepsilon$ model will complicate further the problem and increase the required computer resources.
- The problem has at least two varying length scales; a small nozzle diameter and a large tank dimension.

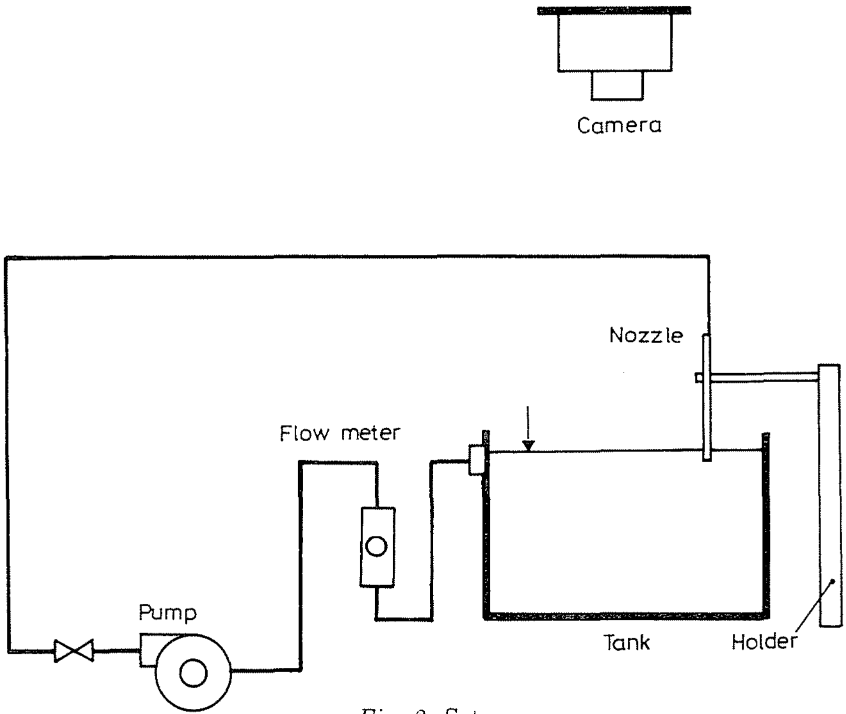

Fig. 2. Setup

2. Flow Visualization and Measurement

In the experimental study visual observation of light particles floating on free surface of the water and suspended particles circulating with the flow or settling on the bottom indicated that the flow may be treated as axisymmetric for some cases. The inclined jet with its axial downward and tangential components produces a swirling motion in the sense defined previously. This observation was utilized to device a simple flow model for the complex problem. A method based on imaging streamlines and using computer digitization was developed and used for measuring the distribution of the tangential velocity on the free surface (details are given in [10]). A typical image taken by the camera on *Fig. 2* is shown in *Fig. 9.*

3. Distribution of the Tangential Velocity

Based on observation we attempt to find some simple solutions that may give further insight into the nature of the problem and indicate possible simplification to reduce its complexity. A natural start is to use one of the existing models. LITVAI and HEGEL [5] used *Eq.* (13) to predict the tangential velocity distribution using the distance from the centre of the tank to the location of the jet (r_1) for r^*. They tested this assumption for a single set of data and their tuning of constants for the friction coefficient cannot be generalized. However, this assumption was not always suitable. Additionally, the equation does not provide for any systematic way to treat all sets of data. In what follows we reconsider the derivation starting from the Navier-Stokes equations with somewhat different non-dimensional regrouping of the variables.

3.1. Mathematical Analysis

The Navier-Stokes equation for the tangential velocity component for axisymmetric incompressible flow is:

$$\frac{V_r}{r}\frac{\partial(rV_\theta)}{\partial r} + V_z\frac{\partial V_\theta}{\partial r} - \nu_{eff}\left[\frac{\partial}{\partial r}\left(\frac{1}{r}\frac{\partial(rV_\theta)}{\partial r}\right) + \frac{\partial^2 V_\theta}{\partial z^2}\right] = 0\,, \tag{4}$$

where $v_{eff} = v_{tur} + v_{lam}$ is assumed to remain constant; turbulence is assumed to increase in effect the normal molecular viscosity [5, 7]. If V_θ is assumed to be independent of z the partial differential equation simplifies to an ordinary solvable one

$$\frac{V_r}{r}\frac{\mathrm{d}rV_\theta)}{\mathrm{d}} - \nu_{eff}\mathrm{dd}\left(\frac{1}{r}\frac{\mathrm{d}rV_\theta)}{\mathrm{d}}\right) = 0\,. \tag{5}$$

If we introduce the following non-dimensional parameters:

$$\lambda = \frac{V_{r2}r_2}{\nu_{eff}}\,, \tag{6}$$

$$\Gamma^* = \frac{V_\theta r}{V_{\theta 2} r_2}\,, \tag{7}$$

$$R = \frac{r}{r_2}\,, \tag{8}$$

where r_2 is the tank radius and $V_{\theta 2}$ is the corresponding tangential velocity. In order to solve the differential equation we need to know V_r. As a first approximation we assume that V_r is proportional to r. This assumption is suggested by experiment. The solution may be assumed of the form:

$$\Gamma^* = \frac{c_1}{\lambda} - c_2\epsilon^{-\frac{\lambda}{2}R^2}\,. \tag{9}$$

Applying the boundary conditions $\Gamma^* = 1$ at $R = 1$ and $\Gamma^* = 0$ at $R = 0$, we obtain:

$$c_2 = \frac{1}{1 - e^{-\lambda/2}} \tag{10}$$

and

$$\frac{c_1}{\lambda} = c_2 \,. \tag{11}$$

Hence the final solution is:

$$\Gamma^* = \frac{1 - e^{-(\lambda/2)R^2}}{1 - e^{-\lambda/2}} \tag{12}$$

or

$$V_\theta = \frac{V_{\theta 2} r_2}{1 - e^{-\lambda/2}} \frac{\left(1 - e^{-(\lambda/2)R^2}\right)}{r} \tag{13}$$

Comparison to *Eq.* (2) reveals that:

$$k_1 = \frac{V_{\theta 2} r_2}{1 - e^{-\lambda/2}} \tag{14}$$

and

$$k_2 = \frac{\lambda}{2 r_2^2} \,. \tag{15}$$

3.2. Determination of λ

We plot *equation* (12) for various values of λ and then superimpose Γ_e^* (Γ^* calculated from experiment) on the same graph. Values of $(rV_\theta)_2$ required to put the experimental circulation (Γ_e) into a non-dimensional form (Γ_e^*) were extrapolated from experimental trend curves and adjusted to give the best possible fit. *Fig. 3* displays the results. The theoretical non-dimensional circulation (Γ^*) fits very well the measured one (Γ_e^*) with a single value of $\lambda = 8$ and for unique values of $(rV_\theta)_2$ for each set of data. These values are given in *Table 1*.

Table 1. Values of k_1 and k_2 for best fit of experimental data

Set #	k_1	$V_{\theta 2}$	k_2
p293	0.035	0.043	6.25
p592	0.060	0.074	6.25
p992	0.130	0.159	6.25

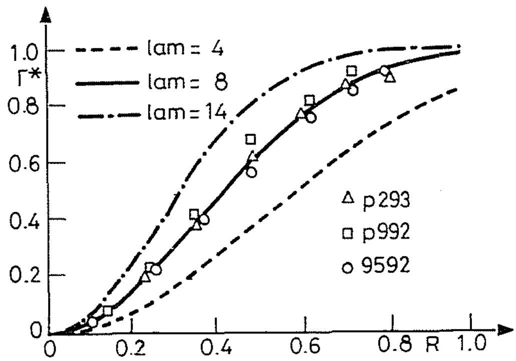

Fig. 3. Determination of λ

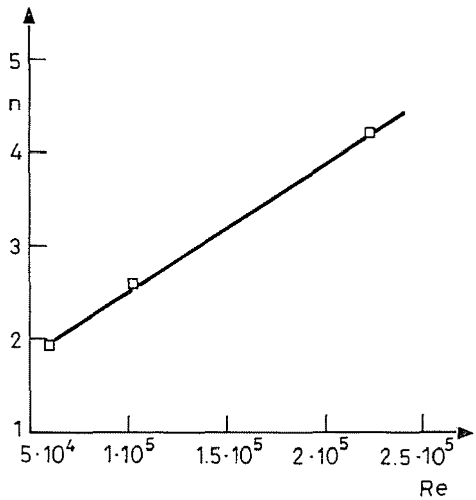

Fig. 4. Relation of power law exponent n and Re for best fit of experimental data

3.3. Estimation of $V_{\theta 2}$

To determine $V_\theta(r)$ from design and operational parameters, we need to find $V_{\theta 2}$. In equilibrium, the momentum produced by the tangential component of the jet is balanced by frictional forces acting on the walls of the tank. An angular momentum balance over the total volume yields:

$$M_{Jet} = M_{side-wall} + M_{floor} \,. \tag{16}$$

where M_{Jet} is the rate of convection of angular momentum by the tangential component of the jet. M_{floor} and $M_{side-wall}$ are the momentum dissipated by the side and bottom of the tank

$$M_{Jet} = \rho\pi v_j^2 r_n^2 r_1 \sin\theta\,, \tag{17}$$

$$M_{side-wall} = 2\pi r_2^2 h \tau_{r\theta} = \rho\pi C_{f,s} h r_2^2 V_{\theta 2}^2\,, \tag{18}$$

$$M_{floor} = \rho\pi \int_0^{r_2} C_{f,b} v_\theta^2 r^2 \mathrm{d}\,, \tag{19}$$

v_j is the velocity of the jet at the nozzle exit, r_n is the nozzle radius, r_1 is the position of the jet from the center of the tank and θ is the nozzle angle of inclination, r_2 is the tank radius, and h is the tank height. The shear stress $\tau_{r\theta}$ was replaced by

$$\tau_{r\theta} = \frac{\rho}{2} v_\theta^2 C_f\,, \tag{20}$$

where C_f is a friction coefficient. Substitution in the momentum balance equation yields:

$$v_j^2 r_n^2 r_1 \sin\theta = C_{f,s} h r_2^2 V_{\theta 2}^2 + \int_0^{r_2} C_{f,b} v_{\theta,b}^2 r^2 \mathrm{d}\,. \tag{21}$$

The calculation of the contribution to the momentum equation by the floor is complicated by the dependence of both $C_{f,b}$ and $v_{\theta,b}$ on r. If we assume that $v_{\theta,b}$ has the same distribution as that at the free surface multiplied by a decay factor then *Eq.* (21) may be solved exactly or numerically. Thus:

The formulae available for calculating C_f for pipes or flat plate over-predict the peripheral tangential velocity that fit best the experimental data. When the constants in the power law equation were modified to predict the desired value of $V_{\theta 2}$ for one set, the prediction improves but better accuracy is still desirable. There are good reasons for this to happen. The nature of the problem is different from those in pipes or flat plates and the tangential velocity decays towards the floor. An effective friction-like factor accounting for these factors and other unknown ones is to be sought. The friction factor f is a function of the exponent n in the power law.

$$f = \frac{c}{n^2} \tag{23}$$

and

$$C_f = \frac{f}{4} = \frac{0.3}{n^2}\,, \tag{24}$$

where $c = 1.2$ is used according to HINZE [4]. The exponent n is a function of the Reynold's number, e.g. $n = 6$ at $Re_D = 4\cdot 10^4$ and $n = 9$ at $Re_D = 10^6$ [4, 6]. By trial and error, n was selected to produce the desired C_f for the three data sets under investigation. The resulting values are plotted versus

Re in *Fig. 4*. The points lie on a straight line. By regression analysis, the following relation was obtained.

$$n = 1.149 + 1.367 \cdot 10^{-5} Re\,. \tag{25}$$

C_f versus Re is plotted in *Fig. 5*. By looking at the Moody diagram, it is seen that behavior of this system is similar to that of rough pipes in the complete turbulence state. A regression fit for C_f in terms of Re is also found:

$$C_f = 0.3874 \cdot 10^5 Re^{-1.184}\,. \tag{26}$$

There seems to be a good correlation for the investigated sets of data.

3.4. *Simple Closed Form Solution*

Having found ways to determine $V_{\theta 2}$ in general we now seek a simple closed form solution relating it to operational parameters. Assuming C_{fb} constant and equal to C_{fs}, momentum lost on the floor is approximated as follows:

$$M_{floor} = \rho\pi C_{fb} k_1^2 \int_0^{r_2} \left(1 - e^{-6.25r^2}\right)^2 \mathrm{d} \approx$$

$$\rho\pi C_{fb} k_1^2 [0.251 \mathrm{erf}(3.54 r_2) - 0.71 \mathrm{erf}(2.5 r_2) + r_2]\,. \tag{27}$$

The expression in square brackets may be simplified further to $[r_2 - 0.455]$ for r_2 larger than 0.7. Introducing these simplifications we obtain:

$$V_{\theta 2} = \left[\frac{0.25 v_j^2 d_n^2 r_1 \sin\theta}{0.3874 \cdot 10^5\,(h + 0.2(r_2 - 0.455))}\right]^{1.225} \left(\frac{2}{\nu}\right)^{1.45}\,. \tag{28}$$

4. Estimation of the Eddy Viscosity

In deriving *Eq.* (13) for the distribution of the tangential velocity, it was assumed that the viscosity is constant; the turbulence is assumed to increase the effective viscosity in a manner that the eddy viscosity may be treated, on the average, as a constant. This assumption was utilized in applications mentioned previously, in which Burgers' solution was used to fit experimental data. Useful information on the computation of constant effective eddy viscosity is found in [1]. The eddy viscosity was found to correlate with Re as follows:

$$\frac{\nu_e}{\nu} = \frac{Re}{Re_{\min}}\,. \tag{29}$$

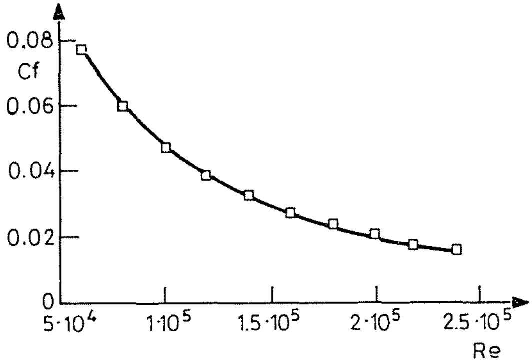

Fig. 5. Relation of C_f to Re for best fit of experimental data

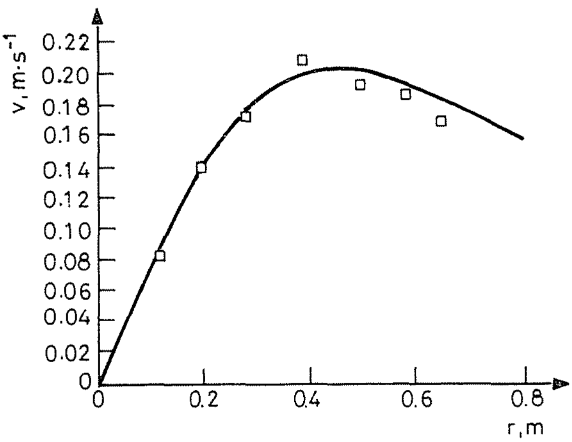

Fig. 6. Comparison of predicted and measured tangential velocity profile for v_j = 19 m/s, $d_n = 5.1$ mm, $r_1 = 0.34$ m, and $\theta = 30°$

Re is based on the maximum tangential velocity and the corresponding radius. $Re_{\min}$ is equal to 30. This relation was found by order of magnitude analysis and verified by experiment.

5. The Constant Eddy Viscosity Model

Now we have all the ingredients to formulate a more elaborate mathematical model. With the tangential velocity at the free surface as a boundary condition and the effective velocity producing it known, it is possible to calculate the flow field in the rest of the tank by the numerical solution of the axisymmetric Navier-Stokes equations. The measured profile of the tangential velocity accounts of the effect of the jet.

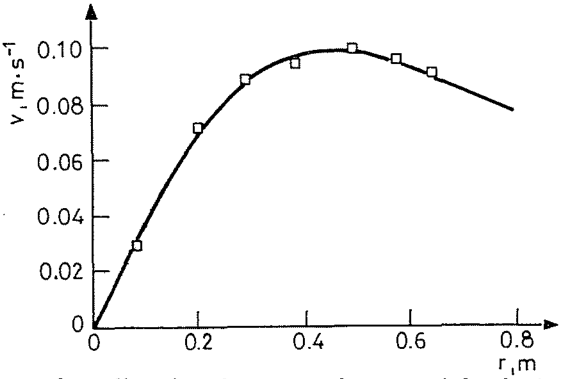

Fig. 7. Comparison of predicted and measured tangential velocity for $v_j = 9$ m/s, $d_n = 5.1$ mm, $r_1 = 0.54$ m, and $\theta = 30°$

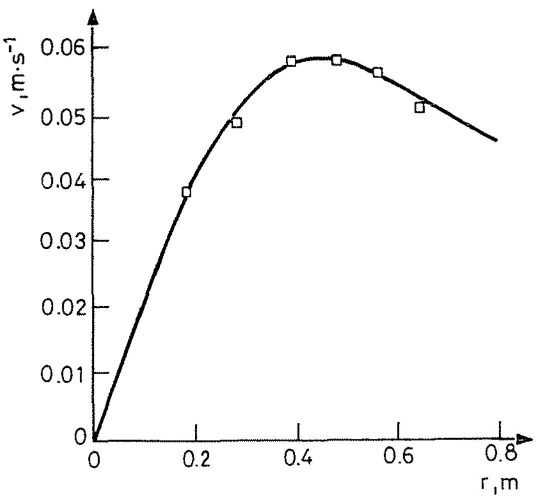

Fig. 8. Comparison of predicted and experimental data for $v_j = 1.84$ m/s, $d_n = 25$ mm, $r_1 = 0.33$ m, and $\theta = 30°$

6. Conclusions

We have formulated a simple mathematical model for the prediction of the tangential velocity on the free surface. With some information about the decay of swirl velocity it is possible to generalize the model to the whole flow field. We summarize the main findings in the following points:

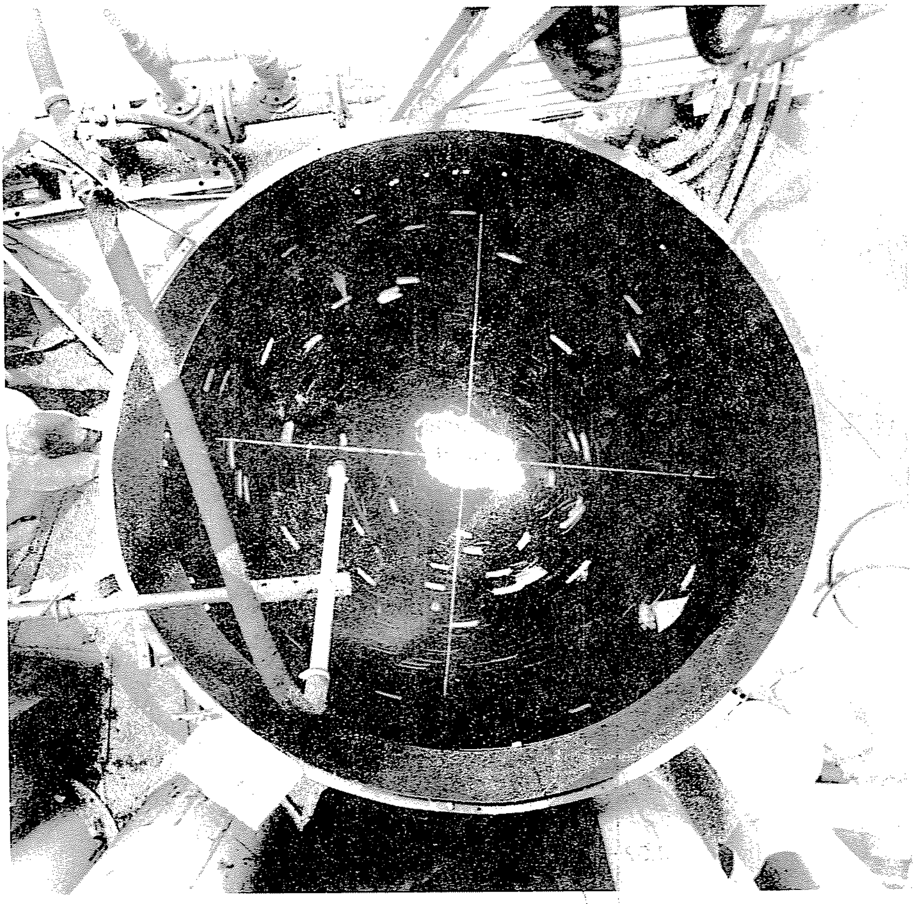

Fig. 9. A typical image by the camera on *Fig. 2*

1. The derived model was found to fit the experimental averaged tangential velocity profile remarkably well for the three tested sets of data by a single parameter $\lambda = 8$ provided that the tangential velocity at the periphery is well predicted.

2. The tangential velocity at the periphery was calculated from a momentum balance on the radial component of the jet. A close form simple formulae relating $V_{\theta 2}$ to design and operational parameters was derived.

3. A constant viscosity model with the tangential velocity profile at the free surface (accounting for the effect of the jet) as a boundary condition is proposed.

References

[1] ALBRING, W. (1981): Elementarvorgänge fluider Wirbelbewegungen, Akademie-Verlag, Berlin.
[2] BURGERS, J. (1948): A Mathematical Model Illustrating the Theory of Turbulence, in Advances in Applied Mechanics, Vol. I., Academic Press, N.Y. 198.
[3] ESCUDIER, M. (1987): Confined Vortices in Flow Machinery, *Ann. Rev. Fluid Mech.*, Vol. 19, p. 27.
[4] HINZE, J. (1975): Turbulence, 2nd ed. McGraw-Hill, New York.
[5] LITVAI, E. – HEGEL, I. (1991): A Simple Theory for the Jet-Driven Flow in a Cylindrical Tank, *9th Conf. on Fluid Machines*, Budapest, p. 226.
[6] POTER, M. – WIGGERT, D. (1991): Mechanics of Fluids, Prentice-Hall International.
[7] RODI, W. (1984): Turbulence Models and Their Application in Hydraulics, IAHR.
[8] ROTT, N. (1958): On the Viscous Core of a Line Vortex, *ZAMP*, Vol. IXb, p. 543.
[9] KURODA, C. – OGAWA, K. (1986): Turbulent Swirling Pipe Flow, in The Encyclopedia of Fluid Mechanics, N., P. Cheremisiolf. Editor, Vol. 6, Gulf Publishing Co.
[10] TUWEGIAR, I. (1996): Numerical and Experimental Investigation of Jet-Induced Flow in Cylindrical Tanks, PhD Dissertation.